

Evaluation of Soil Liquefaction Potential around Enfidha International Airport, Tunisia

Hatem Gasmi^{1,2}

¹College of Engineering, University of Ha'il, Hail, Kingdom of Saudi Arabia

² Geotechnical Engineering Research laboratory, University of Tunis El Manar, Tunisia

E-mail address: gasm_i_hatem@yahoo.fr

ABSTRACT

During this last century, the examples of liquefaction caused by the earthquakes are very numerous and their consequences are responsible for several important damages. Thus, several countries are currently facing this problem and search to improve their structure design against the earthquake.

In this paper, we are interested in studying the area of Enfidha Airport, given its strategic and economic importance in the Mediterranean basin. In order to do this, and before practicing the liquefaction evaluation method, it is primordial to present the geological and seismic setting of area studied.

This research work aims to highlight the methods of recognition and to evaluate as a case study the liquefaction of the Enfidha zone using the empirical relationships between the Standard Penetration Test (SPT) and the Cone Penetration Test (CPT).

The study showed the serious existence of liquefaction risk in some areas. Thus, the liquefaction potential index values were interpreted and compared; it was observed that there was not a perfect agreement between the results of the two tests. The liquefaction potential index values using the SPT were found to be lower than those of the CPT method.

Keywords: earthquakes; liquefaction potential; Geotechnical Investigations; Enfidha International Airport

1. INTRODUCTION

The soils liquefaction is an instability phenomenon or loss of resistance that can generally take place on a granular saturated or partially saturated medium. It is manifested by an increase in pore pressure linked to the contracting behavior of the soil during the application of swift loading (earthquake, shocks, tidal waves...). The liquefaction phenomenon is at the origin of a sudden instability of soils which flowing under the effect of gravity and the loads can cause irreparable damage to nearby structures.

After the earthquake of Alaska (1964) and Niigata in Japan (1964), Seed and Idriss (1971) developed a simplified procedure based on field tests for the evaluation of liquefaction potential. Subsequently, this procedure has undergone several modifications or improvements, notably by Seed (1979), Seed and Idriss (1983), and Seed *et al.* (1985).

In January 1996, a workshop on liquefaction problems was organized by the National Center for Earthquake Engineering Research (NCEER); the recommendations of this workshop are analyzed by Youd *et al.* (2001). Currently, the liquefaction study has developed to become a completely separate area of research (Andrusa *et al.*, 2004; Monaco *et al.*, 2005; Grasso and Maugeri, 2006; Tsai *et al.*, 2009).

Generally, cyclic shear stresses could be assessed through simplified procedures (Seed, 2010) or based upon results of a site response analysis. The cyclic shear resistance of soils could be evaluated in the laboratory or based upon empirical relationships using in-situ material parameters e.g., SPT, CPT, or Vs (Finn, 2002; Ali *et al.*, 2014; Shelley *et al.*, 2015).

Pathak and Dalvi (2011) have already developed similar such model “model A” separating “yes “ and “ no” zones of liquefaction based on field performance data. Further, these authors have also invented a method to evaluate triggering acceleration indicating initiation of liquefaction.

Numerous cases of runoff, cited in the literature, in natural soil media and artificial structures, have been attributed to liquefaction, for example: Fort Peck Dam (1938), Niigata in Japan (1964), Moss Landing, California (1989), Chi-Chi, Taiwan (1999), Adapazari, Turkey (1999), Boumerdes, Algeria (2003), Christchurch, New Zealand (2011), ...

Soil liquefaction can therefore result from seismic stress; the induced deformations, even moderate, can render certain structures unfit. Hence the interest of seriously examining the liquefaction potential of a given site, in this case Tunisia, knowing that this phenomenon was observed during the Sidi Thabet earthquake of 1 December 1970 for a moderate magnitude of 5.1. Since this event, the government has given increasing importance to this phenomenon especially as regards the mega projects that is the case of Enfidha International Airport.

The purpose of this project is therefore to identify the underground liquefaction potential of Enfidha city, using the most current methods.

2. STUDY AREA

2.1 Geographical setting

The study area is part of northeastern Tunisia. It is approximately between 10 ° and 11.5 ° south latitude and between 35 ° and 36.30 ° east longitude. It is bounded on the west by the Zaghouan faults corridor which separates it from the Atlas domain. In this region, from south to north we find the following structures: Jebel Souatir, Fadhloun, Garci, Mdeker, the eastern flank of the Saouaf syncline, the massifs between Jradou and Takrouna.

2.2 Geological setting and Seismicity of the region

The study area includes the Enfidha block in the North which corresponds to a folded and faulted zone. According to Burolet (1981), the geological structures of Enfidha are closely linked to the North-South axis. This axis corresponds to a deep suture due to the heterogeneities of the base. It separates an unstable domain in the West and a stable domain in the East. It is considered as a bumper on which are molded and struck the atlastic folds. It is a zone with a great reduction of thickness and many discrepancies.

The region consists of areas that are moderately unstable on the seismic plane. According to the historical seismicity the destructive earthquakes have a periodicity of about four centuries. The liquefaction potential of soils should be examined for PGA within a range from 0.05g to 0.3g.

3. GEOTECHNICAL INVESTIGATIONS

For this study, we have the results of geotechnical surveys carried out on 25 sites. The first step in our work was the consolidation of a geotechnical database including: 105 core drilling; 59 pressuremeter tests; 41 Standard penetration test (SPT); and 58 Cone Penetration Tests (CPT);

The available data are recent and spread over the different areas mentioned above. All data has been stored and managed using RockWorks software, which also provides a representation of the layers in place. Figure.1 shows the location of these data in georeferenced coordinates.

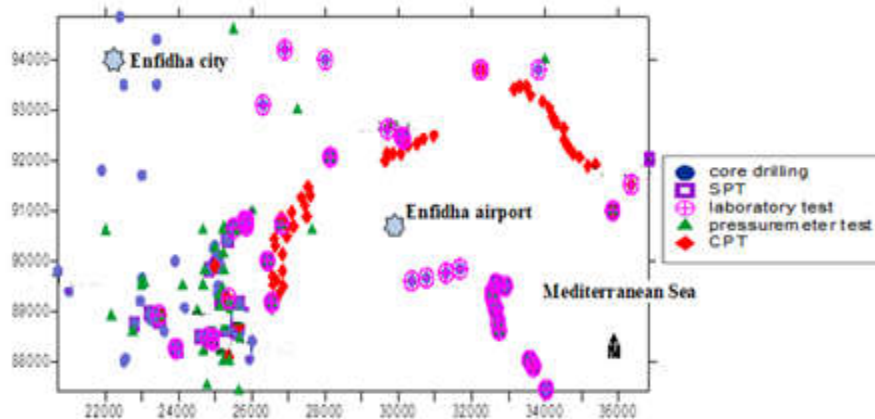


Fig. 1: Location of geotechnical tests

The subsoil of the study area is complex and extremely variable;

The subsoil is chaotic and characterized by a compact clay substratum of variable depth from 10 to 60 m. The layers overlying the substratum are also of varying thicknesses and depths, as shown by subsequent sections made in different areas using RockWorks (Figures 2).

- At Enfidha downtown site (Figure.2.a), we identify (from bottom to top) a layer of tufous clay, a layer of gray plastic clay, an alternation of layers of clay, sand and silt, a thick layer of silt (about 25 m) and finally a superficial layer of backfill.
- Figure.2.b shows a section along the Enfidha airport runway; the following layers are identified (from bottom to top): a layer of reddish clay, a sandstone lens, a layer of sandy yellowish clay, a layer of gray plastic clay, a layer of sandstone sand, alternating layers of clay, sand and silt finally a layer of fill.
- At Enfidha Sea coast, and according to the section shown in Figure.2.c, the subsoil consists from the bottom to the top of: gray plastic clay, a layer of sand then alternating layers of clay and sand silt with sandstone passages, a layer of sand, a layer of silt and finally a superficial layer of backfill.

- As shown in the section of the subsoil located at The Sabkha of Assa Juriba shown in Figure.2.d (from bottom to top), we encounter: a layer of sandstone sand, a layer of sandy yellowish clay and finally a layer of backfill.

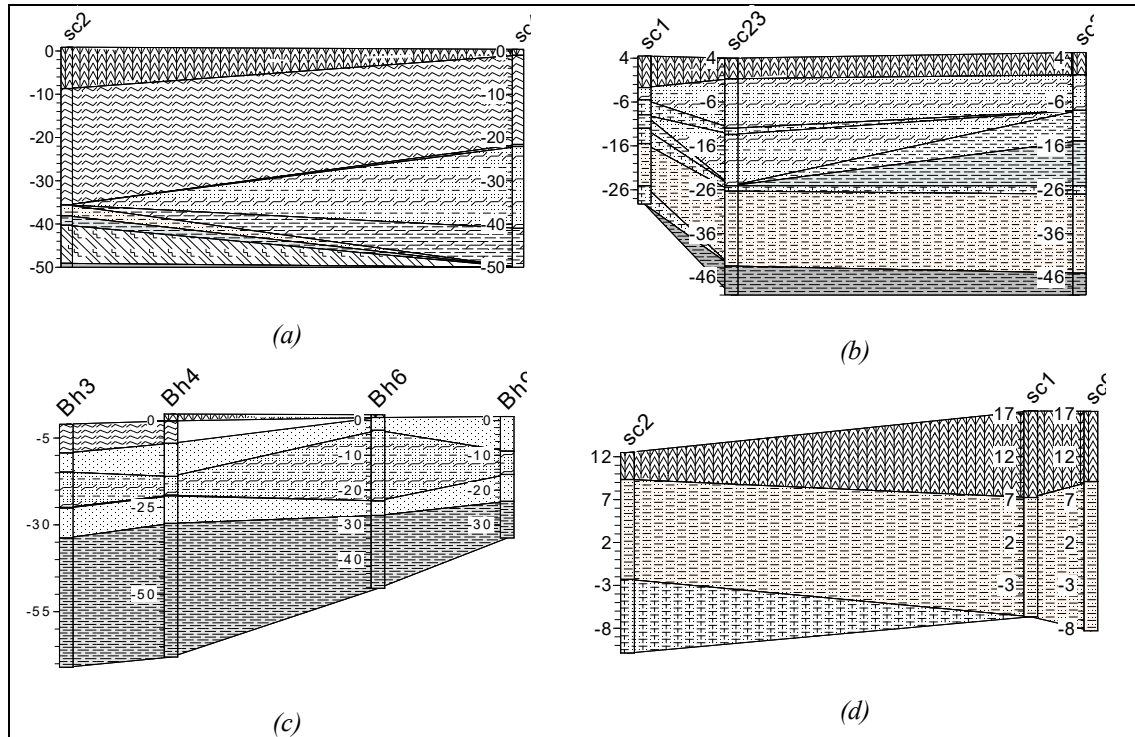


Fig. 2: subsoil cross-section illustrating studied sites: (a) Enfida downtown area; (b) Enfida airport area; (c)Enfida Sea coast; (d) sabkha of Assa Juriba area

4. THE USED METHODOLOGY

The methodology used for this study is inspired by the recommendations of the French Association of Parasismic Engineering (AFPS, 1993) which dictates three levels of evaluation;

4.1. Level A

A first qualitative study of liquefaction sensitivity will result from the exploitation of geological and hydrogeological data as well as soil characteristics independently of the seismic hazard.

4.1.1. Identification of liquefiable soils

The identification is done according to the criteria of Seed *et al.* (2003). These criteria classify soils based on soil index parameters. Soils, which satisfy all three following conditions: (i) $PI < 12$, (ii) $LL < 37$ and (iii) $w_c / LL > 0.8$ fall into Zone A and considered to be potentially liquefiable. Soils lie in Zone B, i.e. satisfying the following conditions: (i) $12 < PI < LL < 47$ and (iii) $w_c / LL > 0.85$, are classified to be moderately susceptible to liquefaction and need further testing. Soils lie out of these boundaries (named as Zone C) are not considered to be susceptible to “classical” liquefaction.

4.1.2. Geological and hydrogeological characteristics of the site

In addition to the criteria outlined above, the following criteria based on geology and piezometric level will be added to assess susceptibility to liquefaction (Table.1).

Table 1: Susceptibility of sedimentary deposits to liquefaction according to the nature and age of the deposit (Seed *et al.* 2003)

Nature of deposit	Possibility of occurrence of liquefaction of saturated powdery soils			
	< 500 ans	Holocene < 10000 years	Pleistocene < 1650000 years	Pre-Pleistocene > 1650000 years
Dépôts continentaux				
River	Very high	High	low	Very low
Alluvial plain	High	Moderate	Low	Very low
Wind deposits	High	Low	Low	Very low
Marine terraces	Moderate	Low	Low	Very low
deltas	-	Moderate	Very low	Very low
Lacustrine deposits	High	Moderate	Low	Very low
colluvial	High	Moderate	Low	Very low
dunes	High	Moderate	Low	Very low
Loess	High	High	High	Inconnue
Glacial moraine	Low	Low	Very low	Very low
Coastal areas				
deltas	Very high	High	Low	Very low
estuaries	High	Moderate	Low	Very low
beaches	Moderate to High	Moderate to Low	Low to Very low	Very low
lagoons	High	Moderate	Low	Very low
Artificial fillings				
Not compacted	Very high	-	-	-
compacted	Low	-	-	-

The purely geological or morphological analyzes make it possible to map the susceptibility of a deposit to liquefaction. Only the consideration of the mechanical characteristics and those of the seismic movement allows a real estimate of the liquefaction potential.

4.2. Level B

Level B studies will use the mechanical characteristics of soils. These studies are based on the comparison between cyclic resistance ratio (CRR) expressed as a function of the mechanical characteristics of soils and the cyclic loading intensity, expressed by the uniform duty cycle stress ratio (CSR).

4.2.1. Cyclic Stress Ratio (CSR)

The expression for the CSR induced by earthquake ground motions formulated by Idriss and Boulanger (2004) is as follows:

$$CSR = \left(\frac{a_{max}}{g} \right) \cdot \left(\frac{\sigma_v}{\sigma'_v} \right) \cdot r_d \cdot \frac{1}{MSF} \cdot \frac{1}{K_\sigma} \times 0.65 \quad (1)$$

the a_{\max} is the peak horizontal ground acceleration; g is the acceleration of gravity; σ_V and σ'_V are total vertical overburden stress and effective vertical overburden stress, respectively, at a given depth below the ground surface; r_d is the depth-dependent stress reduction factor; MSF is the magnitude scaling factor; and K_σ is the overburden correction factor.

For z depth of investigation and M magnitude of earthquake, the stress reduction factor (rd) is given by:

$$\text{If } z \leq 34 \text{ m} \quad \begin{cases} Ln(r_d) = \alpha(z) + \beta(z)M \\ \alpha(z) = -1.012 - 1.126 \sin\left(\frac{z}{11.73} + 5.133\right) \\ \beta(z) = 0.106 - 0.118 \sin\left(\frac{z}{11.28} + 5.142\right) \end{cases} \quad (2)$$

$$\text{If } z > 34 \text{ m} \quad r_d = 0.12 \exp(0.22 M) \quad (3)$$

The magnitude scaling factor (MSF) is as follows:

$$\text{MSF} = 6.9 \exp\left(\frac{M}{4}\right) - 0.058 \leq 1.8 \quad (4)$$

Concerning the overburden correction factor K_σ is given by:

$$\text{- For SPT} \quad \begin{cases} k_\sigma = 1 - C_\sigma \ln\left(\frac{\sigma'_{v0}}{Pa}\right) \\ C_\sigma = \frac{1}{18.9 - 2.55\sqrt{N_{1,60}}} \\ k_\sigma \leq 1.0 \quad \text{and} \quad C_\sigma \leq 0.3 \end{cases} \quad (5)$$

Were Pa is the atmospheric pressure and $N_{1,60}$ is the corrected SPT blow count.

$$\text{- For CPT} \quad \begin{cases} k_\sigma = 1 - C_\sigma \ln\left(\frac{\sigma'_{v0}}{Pa}\right) \\ C_\sigma = \frac{1}{37.3 - 8.27 (q_{c1N})^{0.264}} \\ k_\sigma \leq 1.0 \quad \text{and} \quad C_\sigma \leq 0.3 \end{cases} \quad (6)$$

Were q_{c1N} is the corrected CPT cone resistance

4.2.2. Evaluation of the Cyclic Resistance Ratio (CRR).

- Using SPT:

$$\text{CRR} = \exp\left(\frac{N_{1,60,cs}}{14.1} + \left(\frac{N_{1,60,cs}}{126}\right)^2 - \left(\frac{N_{1,60,cs}}{23.6}\right)^3 + \left(\frac{N_{1,60,cs}}{25.4}\right)^4 - 2.8\right) \quad (7)$$

With $N_{1,60,cs}$ is the number of blows corrected for fine content determined by:

$$N_{1,60,cs} = N_{1,60} + \Delta(N_{1,60}) \quad (8)$$

$$\Delta N_{1,60} = \exp\left(1.63 + \frac{9.7}{FC} - \left(\frac{15.7}{FC}\right)^2\right) \quad (9)$$

With FC is the fines content (in percentage).

- Using CPT:

$$CRR = \exp\left(\frac{q_{C1N}}{540} + \left(\frac{q_{C1N}}{67}\right)^2 - \left(\frac{q_{C1N}}{80}\right)^3 + \left(\frac{q_{C1N}}{114}\right)^4 - 3\right) \quad (10)$$

q_{c1N} is the CPT corrected cone resistance determined by:

$$\left\{ \begin{array}{l} q_{C1N} = \frac{C_N q_c}{P_a} \\ C_N = \left(\frac{P_a}{\sigma'_{v'}}\right)^\beta \leq 1.7 \\ \beta = 1.338 - 0.249(q_{C1N})^{0.264} \end{array} \right. \quad (11)$$

4.2.3. The Safety factor FS

The safety factor results from the comparison of the *Cyclic Stress Ratio* generated by the earthquake and the *Cyclic Resistance Ratio* of the soil.

$$FS = \frac{CRR}{CSR} \quad (12)$$

- $FS \geq 2$: Area not liquefiable
- $1.5 \leq FS < 2.0$: Liquefaction unlikely
- $1.0 \leq FS < 1.5$: Liquefaction likely
- $FS < 1.0$: Almost certainly liquefaction

4.3. Level C

The level C studies are distinguished from level B by the volume of the reconnaissance involved. It is desirable to carry out additional drilling with the completion of SPT and CPT tests. Intact samples will be taken from suspect formations. The cyclic shear stress induced by seismic loading is calculated by dynamic wave propagation calculations.

For these analyzes, the history of representative seismic risk accelerations in a site is used to define the ground movements, in the case of Enfidha according to the seismic hazard: $a_{\max} = 0.05g, 0.1g, 0.15g$ and $0.2g$. For this, we can use specialized software programs of determination of nonlinear site response, such as SUMDES (Li *et al.*, 1992), D-MOD (Matasovic, 2004), NERA (Bardet and Tobita, 2001) and Dissim (Gasmi *et al.*, 2014).

Once the value of the equivalent stress is obtained, we repeat the same calculations performed at level B (Cyclic Stress Ratio and Cyclic Resistance Ratio, finally a safety factor).

5. RESULTS AND DISCUSSIONS

5.1. Study according to level A

5.1.1. Identification of liquefiable soils

The samples available and exploited for this level of study are taken exclusively in clay soils. These samples are taken at different depths; we have therefore represented the results spatially in a georeferenced 3D diagram (figure.3.a). The green color indicates non-liquefiable soil, the red color indicates a confirmed risk of liquefaction, and the blue color represents soils that require further investigation.

The results of the identification of liquefiable soils according to level A are shown in figure.3.b and showed that:

- The majority of the samples examined are non-liquefiable (shown in green);
- Some samples proved to be liquefiable (points in red) at the Enfidha city: the museum area (at depths of 1.5m and 11m), at the gates of the city (depth 19m), the hospital area (depth 31m), airport (depth 16m) and seaside (depth 8m and 13m).
- Other samples (shown in blue) require extensive studies.

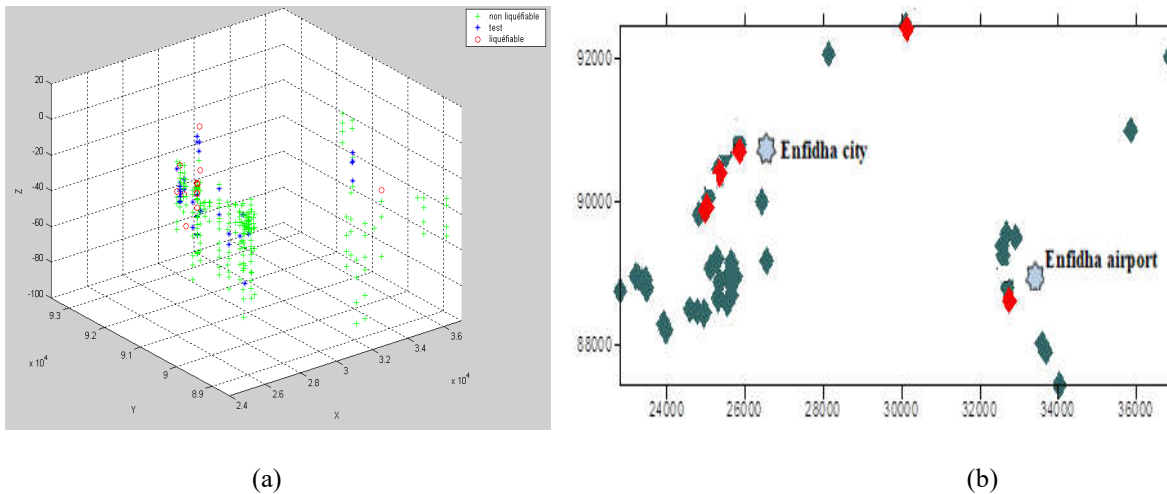


Fig. 3: liquefaction risk based on level A identification: (a) georeferenced 3D diagram; (b) Sample location (Sites with a confirmed risk of Level A liquefaction are shown in red)

5.1.2. Geological and hydrogeological characteristics of the site

In the level A study, we referred to geotechnical zoning studies of the area and dating of shallow muds. Imed Hezzi (2014) dated the muddy surface formations (first 7 meters) as follows (bottom to top):

- A layer of sandstone dating back 8000 years deposited in the middle of Sabkha.
- A layer of greenish-gray mud dating back to 6900 years corresponding to a deposit in an open marine environment.
- A layer of gray and greenish mud dating from 3130 years.
- Finally, a final layer of mud of later age (thickness: 1.5 m).

In term of sedimentological, a 7m thick mud deposit in 8000 years corresponds to an average annual rate of 0.9 mm.

The geotechnical zoning has given the following results:

Table 2: Results of the level A study

Geotechnical zone	Depth of layers	origin	Age of deposit (years)	Susceptibility to liquefaction from	
				Age of deposit	The age of the deposit and the depth of the water table
Zone I	de 0 à 5 m	backfill	from 0 to 700	low	High
	de 1 à 20m	lagoon	from 1000 to 20000	moderate	High
Zone II	de 0 à 15m	alluvial	Pleistocene	low	very low
Zone IV	de 0 à 20m	alluvial	Holocene	moderate	moderate
Zone V	de 0 à 15m	lagoon	pre-pleistocene	very low	very low

5.2. Study according to level B

Susceptibility to liquefaction was examined for maximum surface accelerations of 0.1g to 0.3g; It is represented by the safety factor $FS = \frac{CRR}{CSR}$ calculated step-by-step using Worksheets in Excel, the results are recorded (1) spatially in a 3D georeferenced diagram and (2) by means of sections made in a GIS environment, at different depths up to 20m ($z = 0, -5, -10, -15, \text{ and } -20\text{m}$).

We consider Bh1 test as a calculation example at the airport runway for $a_{\max} = 0.2\text{g}$ and $M = 5.6$. As shown in Table.3, we start the study by introducing the necessary data into an Excel Worksheets (pink ranges): a_{\max} , magnitude, SPT number of blows, corresponding depth, water table level, soil density, material characteristics and percentage in fine. After a step-by-step calculation, the value of the safety factor for a given depth and the susceptibility to liquefaction according to the study at level B (range in orange) are obtained.

The results were represented in an S.I.G environment using ArcView. Some examples for Risk of liquefaction estimated according CPT and SPT are given in Figure.4.

In conclusion, level B studies have shown the presence of layers of sand that can liquefy; they are located in superficial formations characterized by an alternation of clay sand and mud. We have shown that the risk of liquefaction increases with the maximum acceleration on the soil surface (a_{\max}), knowing that it varies between 0.2g and 0.3g for return periods ranging from 200 to 500 years.

Table 3: Excel worksheet calculating susceptibility to liquefaction using the SPT test according to level B

SPT		amax = 0,214	g												
		M = 6,8													
		Pa = 1	atm												
sondage	N SPT	Z (m)	eau nappée	humide(K)	N1	matériel***	N1_60	ss(%)<=0.074	N1_60.cs	CSR	RCC	FS	liquéfaction		
Bh01	2	1	0,7	19,8	3,4	0,975	3,315	44	8,91706528	0,13588741	0,1106561	0,81432193	L quasi certain		
	2	2	0,7	19,8	3,4	0,975	3,315	44	8,91706528	0,1695818	0,1106561	0,65252345	L quasi certain		
	4	3	0,7	19,8	6,8	0,975	6,63	36	12,1548248	0,18335471	0,13361018	0,72869783	L quasi certain		
	4	4	0,7	19,8	6,37056248	0,975	6,21131792	36	11,7361428	0,18969798	0,13050078	0,68793976	L quasi certain		
	3	5	0,7	19,8	4,34811185	0,975	4,23940905	36	9,76423389	0,19238277	0,11642811	0,60518989	L quasi certain		
	1	6,45	0,7	19,8	1,29173566	0,975	1,25944227	36	6,7842671	0,19274092	0,09684789	0,50247707	L quasi certain		
	1	7,45	0,7	19,8	1,18022911	0,975	1,15072338	36	6,67554822	0,19150785	0,09617258	0,50218609	L quasi certain		
	32	8,55	0,7	20,1	32,9277104	0,975	32,1045176	52	37,719177	0,18684196	2,10668046	11,2752002	non liquéfiable		
	6	10	0,7	20,1	5,7740125	0,975	5,62966219	52	11,2443215	0,18379823	0,12690458	0,6904559	L quasi certain		
	12	11,5	0,7	20,1	10,8115199	0,975	10,5412319	52	16,1558912	0,1813903	0,16614564	0,91595659	L quasi certain		
	14	13	0,7	20,1	11,9000533	0,975	11,602552	52	17,2172113	0,17821656	0,17597341	0,98741333	L quasi certain		
	6	14	0,7	20,1	4,73786872	0,975	4,61942201	52	10,2340813	0,17409047	0,11969911	0,68756844	L quasi certain		
	2	15,5	0,7	20,1	1,43515925	0,975	1,39928027	52	7,01393961	0,16867873	0,09828386	0,58266892	L quasi certain		
	6	17	0,7	20,1	4,2001336	0,975	4,09513026	52	9,7097896	0,1648922	0,11605231	0,70380716	L quasi certain		
	4	18,5	0,7	19,2	2,76936726	0,975	2,70013308	95	8,20038201	0,1658914	0,10589938	0,63836567	L quasi certain		
	4	20,5	0,7	19,2	2,58795531	0,975	2,52325642	95	8,02350536	0,15963242	0,10474337	0,65615352	L quasi certain		
	5	22	0,7	19,2	3,11909717	0,975	3,04111974	95	8,54136867	0,15548336	0,10814805	0,6955603	L quasi certain		
	5	23,5	0,7	19,2	2,98549273	0,975	2,91085541	95	8,41110434	0,15139518	0,10728589	0,70864802	L quasi certain		
	100	25	0,7	19,2	96,846021	0,975	94,4248704	95	99,9251194	0,18671152	1,5702E+73	8,4097E+73	non liquéfiable		
Bh02	3	10,5	0,8	19,5	2,88154283	0,975	2,80950426	74	8,37211913	0,18536219	0,10702862	0,57740264	L quasi certain		
	11	12	0,8	19,5	9,94147	0,975	9,69293325	74	15,2555481	0,18286708	0,15828289	0,86556252	L quasi certain		
	5	13,5	0,8	19,5	4,14954831	0,975	4,0458096	74	9,60842447	0,1783486	0,11535442	0,64679185	L quasi certain		
	7	15	0,8	19,5	5,50769853	0,975	5,37000607	74	10,9326209	0,17434822	0,12465583	0,71498193	L quasi certain		
	5	16,55	0,8	19,5	3,65832426	0,975	3,56686615	74	9,12948102	0,16920732	0,11208819	0,6624311	L quasi certain		
	6	19,5	0,8	19,5	3,98823652	0,975	3,88853061	74	9,45114548	0,16029225	0,11427615	0,71292372	L quasi certain		
	60	24	0,8	20,1	47,3239516	0,975	46,1408528	52	51,7555121	0,18532342	2,276,49881	1,2283,9242	non liquéfiable		
	23	25	0,8	20,1	14,3948451	0,975	14,034974	52	19,6496333	0,14738834	0,20166946	1,36828641	L probable		
Bh03 (en mer)	3	7,5	-1,2	17,3	4,40708056	0,975	4,29690355	42	9,8882427	0,26866018	0,11728658	0,43656108	L quasi certain		
	20	9,5	-1,2	17,3	23,4256385	0,975	22,8399976	42	28,4313367	0,25273805	0,40200053	1,59058176	L peu probable		
	19	11,5	-1,2	17,3	20,6375775	0,975	20,1216381	42	25,7129772	0,23837609	0,30792525	1,29176229	L probable		
	11	13,5	-1,2	17,3	11,1632858	0,975	10,8842037	42	16,4755428	0,22505012	0,16903632	0,75110524	L quasi certain		
	6	15	-1,2	18,6	5,17636595	0,975	5,0469568	96	10,5444697	0,19986453	0,12188761	0,60985114	L quasi certain		
	8	20	-1,2	18,5	5,86364692	0,975	5,71705575	95	11,2173047	0,1796849	0,12670874	0,7051719	L quasi certain		
	59	24,5	-1,2	18,5	49,2026558	0,975	47,9725894	97	53,4673925	0,19771841	9681,23893	48964,7835	non liquéfiable		
	67	25,5	-1,2	18,5	57,0612297	0,975	55,634699	97	61,129502	0,19670725	61853472,6	314444300	non liquéfiable		
Bh04	1	4	0,5	19,8	1,7	0,975	1,6575	44	7,25956528	0,1982816	0,09983347	0,50349338	L quasi certain		
	1	6	0,5	19,8	1,37914897	0,975	1,34467025	44	6,94673553	0,19900345	0,09786237	0,49176221	L quasi certain		

5.3. Study according to level C

For the C level study, the risk of liquefaction was examined for different levels of solicitations from a deterministic study of seismic hazard in the region.

The estimation of the induced ground shear stresses will be done by means of a one-dimensional seismic analysis which considers a viscoelastic behavior of the formations in place. The calculation was done using the software EERA (EERA, 2000); it provides the stress levels induced by the earthquake along the lithostratigraphic section considered. These results allow the estimation of the safety factor FS. An example of calculation is given.

The computational accelerogram is that of the Monastir earthquake, which occurred on October 18, 2013 and has duration of 16.6 seconds (recorded with a sampling rate of 0.005s); the maximum acceleration is calibrated to respective maximum levels of 0.05g, 0.1g, 0.15g, 0.2g and 0.3g in accordance with the levels expected by the deterministic study of the regional seismic hazard.

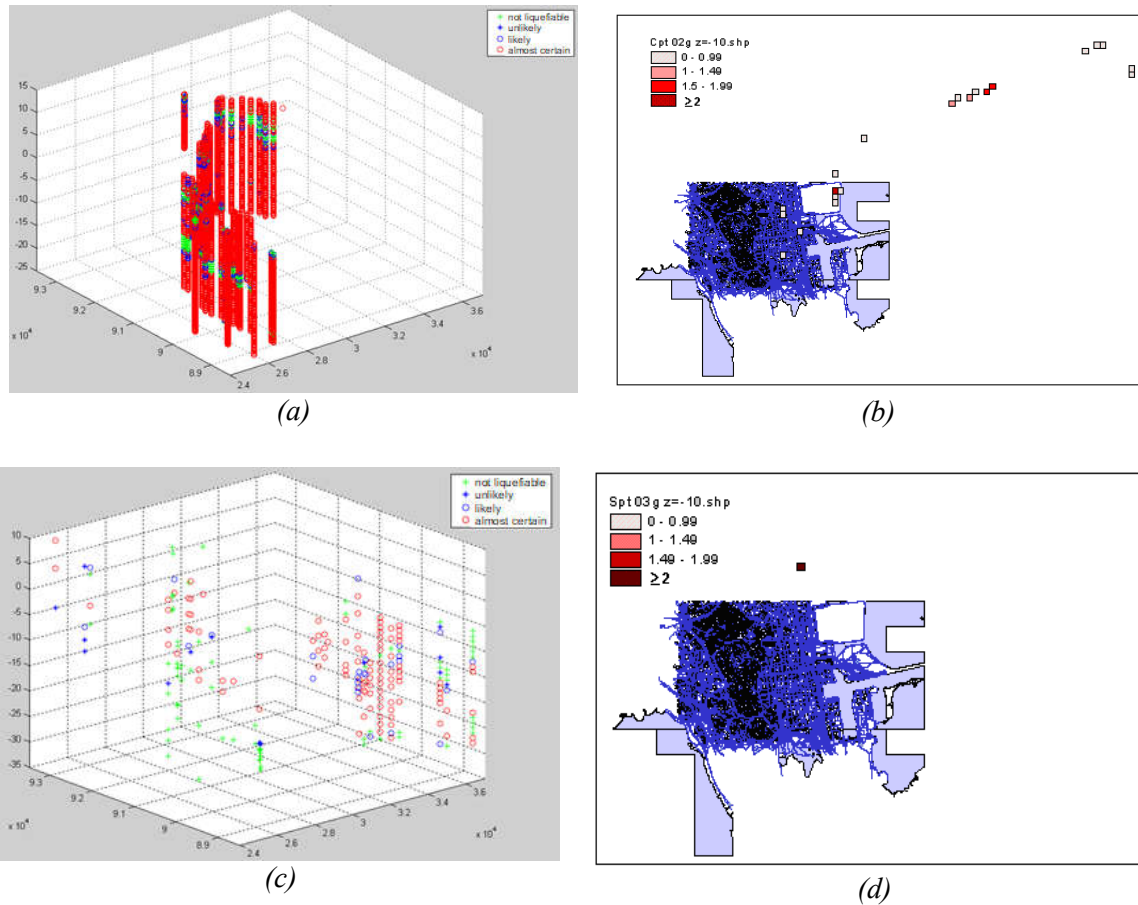
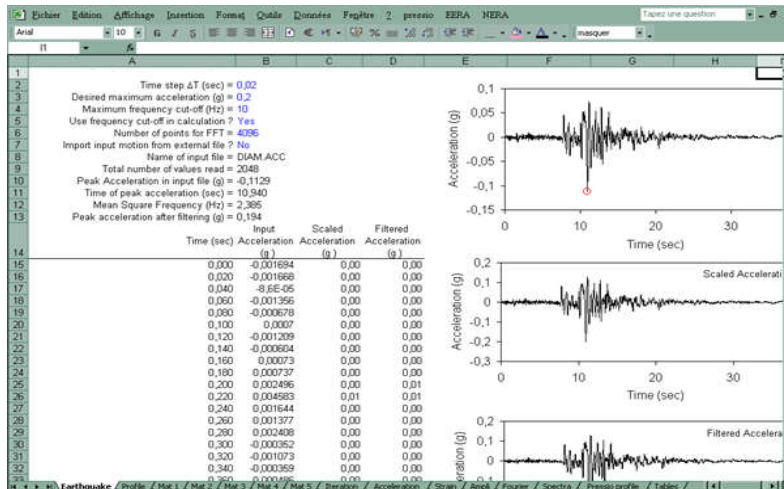


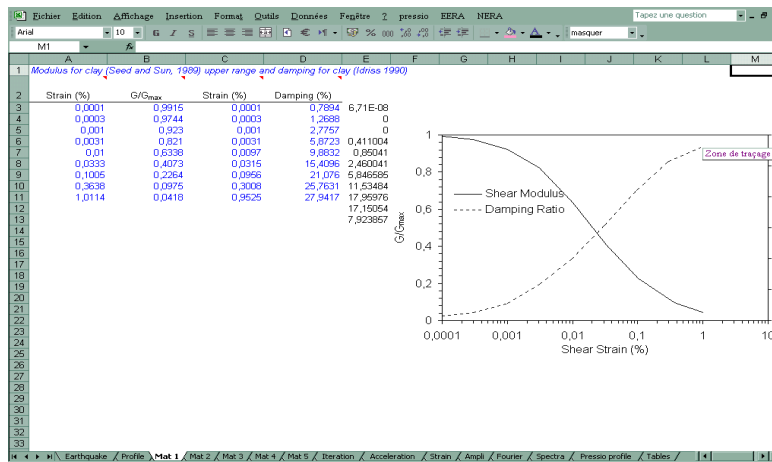
Fig. 4: Risk of liquefaction estimated according to the CPT and SPT test: (a) Risk according to the CPT test spatially in 3D; (b) Risk according to the CPT test at depth $z = -10\text{m}$; (c) Risk according to the SPT test spatially in 3D; (d) Risk according to the SPT test at depth $z = -10\text{m}$

The cyclic shear stress induced by seismic loading is calculated, on some characteristic stratigraphic profiles, by dynamic wave propagation calculations. We begin by introducing the characteristics of the study earthquake and the value of the acceleration of setting (Figure.5.a).

We chose the characteristic profile corresponding to the studied site (pressuremeter test SP5 as an example). We introduced the value of the limit pressure with the corresponding depths as well as the characteristics of the existing layers: materials, thicknesses, and density of the soil. EERA software calculates soil profile characteristics as well as material characteristics from the introduced pressuremeter profile (Figures.5.b).



(a)

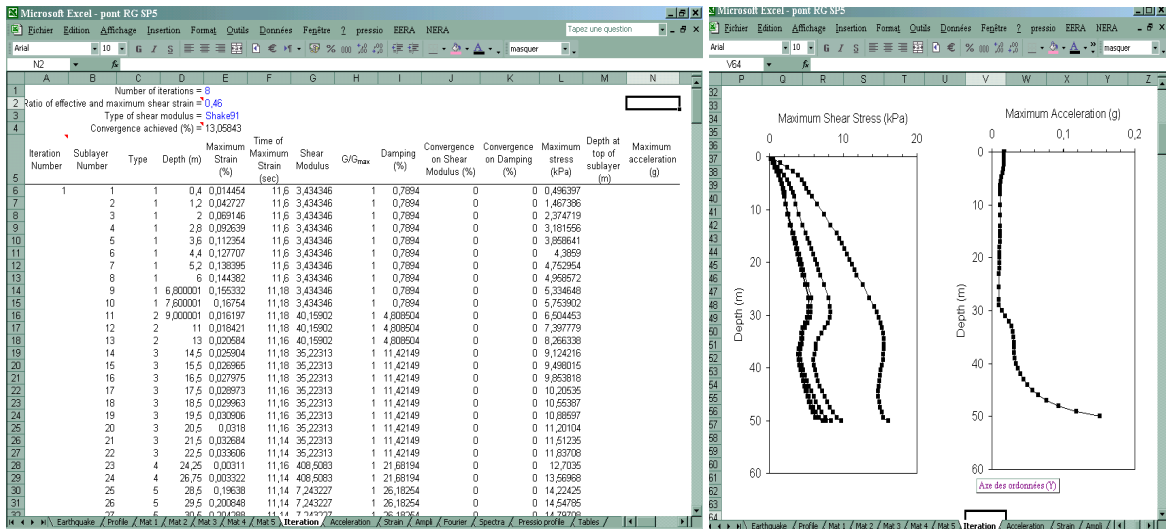


(b)

Fig. 5: characterization of the study site by EERA software: (a) Characteristics of the study earthquake; (b) Characteristics of materials

Once the soil profile and study earthquake characteristics are established, we proceed to the computation of the constraints by the EERA Iteration menu (figures.6).

Once the value of the equivalent linear stress is obtained, the same calculations are repeated at level B; we introduced the maximum shear stress values into the Excel worksheet for each soil depth and recalculated the safety factor values.

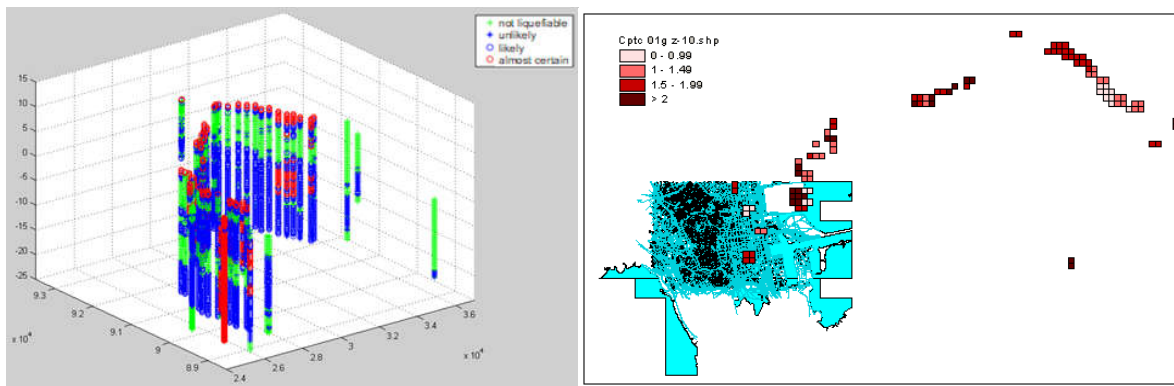


(a)

(b)

Fig. 6: computation of the constraints by the EERA Iteration: (a) Calculation of stresses in a soil profile; (b) Variation of maximum shear stress versus depth and amax value after convergence

The risk of liquefaction at this level C was identified by simultaneously basing on the results of the CPT and SPT tests; the results are presented, as in the studies of previous levels, by means of 3D spatial representations and sections at different depths ($z = 0, -5, -10, -15,$ and -20m). Some examples ($\text{amax} = 0.1\text{g}$) of significant representations of these results are given below (Figure.7).



(a)

(b)

Fig. 7: Liquefaction Risk estimated according to the CPT test (for $\text{amax} = 0.1\text{g}$): (a) spatially in 3D; (b) at depth $z = -10\text{m}$

REFERENCES

- AFPS, (1993) "Guide méthodologique pour la réalisation d'études de microzonage sismique".
- ALI A., ENAN, K., ERMEDIN, T., & BURAK, Y. (2014) Investigation of Soil Liquefaction Potential around Efteni Lake in Duzce Turkey: Using Empirical Relationships between Shear Wave Velocity and SPT Blow Count (N); *Advances in Materials Science and Engineering*, Article ID 290858.
- ANDRUSA, R.D, PARAMANANTHAN, P., BRIAN, S.E, JIANFENG, Z. & HSEIN JUANG, C. (2004) Comparing liquefaction evaluation methods using penetration-VS relationships", *Soil Dynamics and Earthquake Engineering*, 24, 713-721.
- BARDET, J.P. & TOBITA, T. (2001) NERA: A computer program for nonlinear earthquake site response analyses of layered soil deposits, Department of Civil Engineering, University of Southern California, Los Angeles, CA, 43 pp.
- BUROLLET, P.F. (1981) Signification géologique de l'axe nord-sud. Résumés du 1er Congrès Nat. Sc. Terre, Tunis, 31p.
- DALVI, A.N. (2009) Dynamic response analysis of soils due to earthquake-induced liquefaction. M. Tech Dissertation report, Department of Civil Engineering, College of Engineering Pune, Maharashtra, India, pp. 1-67, July 2009.
- EERA, A. (2000) A Computer Program for Equivalent-linear Earthquake site Response Analyses of Layered Soil Deposits. Manuel prepared by J. P. BARDET, K. ICHII, & C. H. LIN.
- FINN W. D (2002) State of the art for the evaluation of seismic liquefaction potential. *Computer Geotechnics*, 29, 328-341.
- GASMI, H., HAMDI, E. & BOUDEN, R.N. (2014) Numerical homogenization of jointed rock masses using wave propagation simulation. *Rock Mech Rock Eng.* 47,1393-1409 DOI 10.1007/s00603-013-0458-8.
- GRASSO, S. & MAUGERI, M. (2006) "Using KD and Vs from seismic dilatometer (SDMT) for evaluating soil liquefaction". *Proc. Second Intern. Flat Dilat. Conf.*, pp. 281-288.
- IDRISS, I.M. & BOULANGER, R.W. (2004) "Semi empirical procedures for evaluating liquefaction potential during earthquakes", *Proceedings of the 11th ICSDEE & 3rd ICEGE*.
- IMED, H. (2014) Caractérisation géophysique de la plateforme de Sahel, Tunisie nord-orientale et ses conséquences géodynamiques. THÈSE/ Université Rennes 1.
- LI, X.S., WANG, Z.L. & SHEN, C.K. (1992) SUMDES: A nonlinear procedure for response analysis of horizontally-layered sites subjected to multi-directional earthquake loading. Dept. of Civil Engineering Univ. of Calif., Davis.
- MATASOVIC, N. (2004) "D-MOD_2 – A Computer Program for Seismic Response Analysis of Horizontally Layered Soil Deposits, Earthfill Dams, and Solid Waste Landfills," User's Manual, Neven Matasovic LLC, Huntington Beach, California.
- MONACO, P., MARCHETTI, S., TOTANI, G. & CALABRESE, M. (2005) "Sand liquefiability assessment by Flat Dilatometer Test". *Proc. 16th Intern. Conf. Soil Mech. and Geo. Engrn.*, Osaka, pp. 2693-2697.
- PATHAK, S.R. & DALVI, A.N. (2011) Performance of empirical Models for assessment of seismic soil liquefaction. *Int. J. Earth Sc. Eng.*, 4, 83-86.
- SEED, H.B. & IDRISS, I.M. (1971) Simplified Procedure for Evaluation Soil Liquefaction Potential. *Journal of Soil Mechanics and Foundation Division ASCE* 97, No. 9, 1249-1273.
- SEED, H.B., IDRISS, I.M. & ARANGO, I. (1983) Evaluation of liquefaction potential using field performance data. *J Geotech Eng, ASCE*, 109,458-482.
- SEED, H.B., TOKIMATSU, K., HARDER, L.F. & CHUNG, R.M. (1985) Influence of SPT procedures in soil liquefaction resistance evaluation. *J Geotech Eng, ASCE* 111(12): 1425-1445.
- SEED, H.B. (1979) Soil liquefaction and cyclic mobility evaluation for level ground during earthquakes. *J Geotech Eng, ASCE*, 105(2), 201-255.
- SEED, R.B., CETIN, M., KAMMERER, W.U., PESTANA, R., SANCIO, B. & KAYEN, F. (2003) "Recent Advances In Soil Liquefaction Engineering : A unified and consistent framework", 26th Annual ASCE Los Angeles Geotechnical Spring Seminar, Keynote Presentation, H.M.S. Queen Mary, Long Beach, California.

- SEED, R.B. (2010) Technical review and comments: EERI monograph “Soil liquefaction during earthquakes” (by Idriss IM, Boulanger RW). Geotechnical report no. UCB/GT-2010/01, UC Berkeley, 75p.
- SHELLEY, E.O., MUSSIO, V., RODRÍGUEZ, M. & JOSÉ, ACOSTA CHANG, G. (2015) Evaluation of soil liquefaction from surface analysis; *Geofísica Internacional*, 54(1), 95-109.
- TSAI, P.H., D.H. LEE, G.T.C. KUNG, & JUANG, C.H. (2009) “Simplified DMT-based methods for evaluating liquefaction resistance of soils.” *Engineering Geology*, 103, 13-22.
- YOU, T.L., I.M. IDRIS, R.D. ANDRUS, I. ARANGO, G. CASTRO & CHRISTIAN, J.T. (2001) Liquefaction resistance of soils: summary report from the 1996 NCEER and 1998 NCEER/NSF Workshops on evaluation of liquefaction resistance of soils. *J Geotech Geoenviron Eng, ASCE*, 127(10),817-833.